PNAS RESEARCH ARTICLE | PLANT BIOLOGY

Ligand diversity contributes to the full activation of the jasmonate pathway in *Marchantia polymorpha*

Sophie Kneeshaw[a], Gonzalo Soriano[a,b], Isabel Monte[a,1], Mats Hamberg[c], Ángel M. Zamarreño[d], Jose M. García-Mina[d], José Manuel Franco-Zorrilla[a], Nobuki Kato[e], Minoru Ueda[e], M[a] Fernanda Rey-Stolle[f], Coral Barbas[f], Santiago Michavila[a], Selena Gimenez-Ibanez[a], Guillermo H. Jimenez-Aleman[a,2,3], and Roberto Solano[a,2]

Edited by Eric Schmelz, University of California San Diego, La Jolla, CA; received February 23, 2022; accepted June 28, 2022 by Editorial Board Member Julian I. Schroeder

In plants, jasmonate signaling regulates a wide range of processes from growth and development to defense responses and thermotolerance. Jasmonates, such as jasmonic acid (JA), (+)-7-*iso*-jasmonoyl-L-isoleucine (JA-Ile), 12-oxo-10,15(*Z*)-phytodienoic acid (OPDA), and dinor-12-oxo-10,15(*Z*)-phytodienoic acid (dn-OPDA), are derived from C18 (18 Carbon atoms) and C16 polyunsaturated fatty acids (PUFAs), which are found ubiquitously in the plant kingdom. Bryophytes are also rich in C20 and C22 long-chain polyunsaturated fatty acids (LCPUFAs), which are found only at low levels in some vascular plants but are abundant in organisms of other kingdoms, including animals. The existence of bioactive jasmonates derived from LCPUFAs is currently unknown. Here, we describe the identification of an OPDA-like molecule derived from a C20 fatty acid (FA) in the liverwort *Marchantia polymorpha* (Mp), which we term (5*Z*,8*Z*)-10-(4-oxo-5-((*Z*)-pent-2-en-1-yl)cyclopent-2-en-1-yl)deca-5,8-dienoic acid (C20-OPDA). This molecule accumulates upon wounding and, when applied exogenously, can activate known Coronatine Insensitive 1 (COI1) –dependent and –independent jasmonate responses. Furthermore, we identify a dn-OPDA–like molecule (Δ^4-dn-OPDA) deriving from C20-OPDA and demonstrate it to be a ligand of the jasmonate coreceptor (MpCOI1–Mp Jasmonate-Zinc finger inflorescence meristem domain [MpJAZ]) in *Marchantia*. By analyzing mutants impaired in the production of LCPUFAs, we elucidate the major biosynthetic pathway of C20-OPDA and Δ^4-dn-OPDA. Moreover, using a double mutant compromised in the production of both Δ^4-dn-OPDA and dn-OPDA, we demonstrate the additive nature of these molecules in the activation of jasmonate responses. Taken together, our data identify a ligand of MpCOI1 and demonstrate LCPUFAs as a source of bioactive jasmonates that are essential to the immune response of *M. polymorpha*.

Marchantia | phytohormone | plant signaling | jasmonate | dn-OPDA

Significance

Plant survival in nature relies on activation of adaptive mechanisms, which largely depends on phytohormones, including jasmonates. Identification of bioactive jasmonates, their biosynthesis, and regulatory mechanisms is a fundamental scientific question. In vascular plants, jasmonates derive from polyunsaturated fatty acids containing 16- or 18-carbons. In contrast, bryophytes are also abundant in C20 and C22 long-chain polyunsaturated fatty acids (LCPUFAs), which are also found in animals. Here, we found that LCPUFAs are also a source of bioactive jasmonates. Using the liverwort *Marchantia polymorpha* (Mp), we discovered a ligand of Coronatine Insensitive 1 (MpCOI1) receptor, investigated its biosynthetic pathway, and showed that the discovered molecule cooperates with dinor-12-oxo-10,15(*Z*)-phytodienoic acid (dn-OPDA), the known MpCOI1 ligand, in the full activation of jasmonate responses in *Marchantia*.

The jasmonate family in plants consists of a subset of oxylipins derived primarily from plastid-derived fatty acids (FAs) (1). Jasmonate hormones activate a plethora of responses involved in the defense, growth, and development of the plant (2, 3). Most studies on jasmonate signaling have been performed in vascular plants, where it has been shown that the bioactive hormone, (+)-7-*iso*-jasmonoyl-L-isoleucine (JA-Ile), is perceived by a coreceptor complex consisting of the F-box protein Coronatine Insensitive 1 (COI1) and a transcriptional repressor Jasmonate-Zinc finger inflorescence meristem domain (JAZ) protein (4–8). JA-Ile–mediated formation of the COI1–JAZ coreceptor triggers the ubiquitination and subsequent degradation of the JAZ, thus allowing for an extensive reprogramming of jasmonate-responsive genes (JRGs) (5, 9). In the bryophyte *Marchantia polymorpha* (Mp), a liverwort that represents a sister lineage to vascular plants, a different ligand, dinor-12-oxo-10,15(*Z*)-phytodienoic acid (dn-OPDA), is perceived by a conserved COI1–JAZ coreceptor complex to activate a similar set of jasmonate responses (10–12). dn-OPDA is a cyclopentenone ring–containing molecule, which in *Marchantia* exists in two major isomeric forms, namely "*cis*" and "*iso*," both of which act as COI1 ligands (10). In addition to binding COI1, dn-*cis*-OPDA, along with the structurally similar 12-oxo-10,15(*Z*)-phytodienoic acid (OPDA), has been shown to have direct signaling capabilities on account of its electrophilic cyclopentenone ring (13–15). These COI1-independent functions of electrophilic jasmonates have been shown to contribute to thermotolerance and are emerging as important to the evolutionary history of plants, likely having played a key role in plants' colonization of land (15).

In the model vascular plant *Arabidopsis thaliana*, the production of JA-Ile occurs through two parallel biosynthetic routes: either from OPDA through the octadecanoid pathway or from dn-OPDA, which is produced from the hexadecanoid pathway

This article is a PNAS Direct Submission. E.S. is a guest editor invited by the Editorial Board.

[1]Present address: Zentrum für Molekularbiologie der Pflanzen (ZMBP), University of Tübingen, 72076, Tübingen, Germany.

[2]To whom correspondence may be addressed. Email: ghj24@cornell.edu or rsolano@cnb.csic.es.

[3]Present address: Molecular Ecology Lab, Boyce Thompson Institute for Plant Research, Cornell University, Ithaca, NY 14850.

This article contains supporting information online at http://www.pnas.org/lookup/suppl/doi:10.1073/pnas.2202930119/-/DCSupplemental.

Published August 29, 2022.

(3, 16). These begin with the lipase-dependent release of C18 (octadecanoid) or C16 (hexadecanoid) ω-3 polyunsaturated fatty acids (PUFAs; α-linolenic acid [ALA; 18:3] and hexadecatrienoic acid [HTA; 16:3]) from plastid membranes. The ALA and HTA molecules are oxygenated by 13- and 11-lipoxygenase (13-/11-LOX) enzymes, respectively, to produce 13- and 11-hydroperoxide intermediates, which then undergo coupled dehydration–cyclization reactions catalyzed by allene oxide synthase (AOS) and allene oxide cyclase (AOC) enzymes, ultimately giving rise to the cyclopentenones OPDA and dn-OPDA (3, 16, 17). Jasmonic acid (JA) synthesis occurs in the peroxisome, where OPDA and dn-OPDA are reduced by the 12-oxo-10,15(*Z*)-phytodienoic acid–reductase 3 (OPR3) enzyme before undergoing three or two successive rounds of β-oxidation, respectively, resulting in the production of (+)-7-*iso*-JA, which may epimerize to the more stable "*trans*" form (−)-JA (18, 19). In addition to the canonical JA biosynthesis, an OPR3-independent route to JA was recently reported, in which OPDA undergoes three rounds of β-oxidation, giving rise to dn-OPDA, tetranor-OPDA, and then, 4,5-didehydro-JA before being reduced by cytosolic OPR1 or OPR2 to produce JA (20). The hormone JA-Ile is formed in the cytoplasm by the conjugation of JA to the amino acid Isoleucine by a JA-amido synthetase, the JA–Resistant 1 enzyme (21). Bryophytes cannot produce JA-Ile and instead utilize both dn-OPDA isomers as COI1 ligands (10, 22, 23). A recent study in *Marchantia* has shown that while a small portion of dn-OPDA comes from octadecanoid pathway–produced OPDA, the main source of dn-OPDA is HTA (i.e., the hexadecanoid pathway) (24).

Despite a reasonably comprehensive understanding of the biosynthetic pathways that give rise to JA-Ile and dn-OPDA, many questions still remain about the breadth and depth of FA-derived signals in plants. This is highlighted by the fact that different plant species exhibit distinct oxylipin signatures: that is, natural differences in the presence and proportions of oxidized FA derivatives (16, 25). PUFAs are generated from saturated FAs through sequential desaturation steps performed by substrate-specific fatty acid desaturase (FAD) enzymes (26). Interestingly, bryophytes, in addition to C16 and C18 PUFAs, possess relatively high amounts of C20 and C22 long-chain polyunsaturated fatty acids (LCPUFAs) along with the corresponding *FAD* genes involved in their synthesis (22, 27). These LCPUFAs, which include arachidonic acid (AA; 20:4n6) and eicosapentaenoic acid (EPA; 20:5n3), are not generally found in vascular plants, but they are present in animals, bacteria, fungi, and algae. AA and EPA are important dietary supplements for animal health (including humans), and as such, recent years have seen an increase in research around their production in plants (27–30). However, very little is currently known about LCPUFA derivatives (e.g., oxylipins) and their potential as signaling molecules in plants. Studies in red algae have identified prostaglandin-like molecules (PGLs) with structural similarity to jasmonates that are derived from AA (31, 32), but while these PGLs were seen to accumulate during immune activation in the alga *Chondrus crispus* (33), experimental limitations in algae hinder a complete dissection of the functional relevance of these molecules. Furthermore, it remains unclear if similar compounds exist in green plant lineages.

A recent study in *Marchantia* has exemplified the need to search for novel PUFA-derived jasmonates. Mutants in the Mp*FAD5* gene were unable to produce HTA and consequently, produced compromised levels of dn-OPDA (24). Given that *Marchantia* plants have no known COI1 ligands besides dn-OPDA, it was interesting to observe that wounded Mp*fad5* plants displayed only minor deficiencies in JRG activation, and the performance of insects (measured as larval weight) fed on Mp*fad5* plants was no different from those fed on wild-type (WT) plants (24). While this could be explained by the low levels of dn-*iso*-OPDA that do accumulate in Mp*fad5* plants, these data could also be indicative of as of yet unidentified signaling molecules that activate the jasmonate pathway alongside dn-OPDA.

In this study, we identify a ligand of COI1, which we name Δ^4-dn-OPDA. We demonstrate this oxylipin to be a dn-OPDA–like molecule derived primarily from the C20 LCPUFA, EPA (20:5n3), via a (5*Z*,8*Z*)-10-(4-oxo-5-((*Z*)-pent-2-en-1-yl)cyclopent-2-en-1-yl)deca-5,8-dienoic acid (C20-OPDA)–like molecule. Our data indicate that Δ^4-dn-OPDA contributes to jasmonate responses in *Marchantia* and offers key insights into the chemical nature and evolution of jasmonate hormones in plants.

Results

Identification of a 20-Carbon OPDA-Like Molecule Derived from EPA. Given that Mp*fad5* mutant plants were not compromised in the activation of jasmonate-related responses, despite having only 5 to 10% of the WT level of dn-OPDA (24), we hypothesized that alternate ligands of COI1 may exist. Several studies have addressed the biosynthetic pathways of n3 and n6 LCPUFAs, such as EPA and AA, in bryophyte plant lineages (*SI Appendix*, Extended Data Fig. 1) (27, 29). However, while it has been demonstrated that C6 and C8 volatiles can be generated from these molecules (34, 35), it is currently unknown if LCPUFAs can act as a source of bioactive jasmonates, as is observed for their C18 and C16 PUFA analogs. Jasmonates accumulate to maximum levels 30 to 60 min after mechanical wounding (36, 37). Therefore, we mined chromatograms (high-performance liquid chromatography–high-resolution mass spectrometry [HPLC-HRMS]) from wounded WT (Takaragaike-1 [Tak-1]) *Marchantia* tissue with the aim of identifying OPDA-like molecules that could derive from C20 LCPUFAs—that is, cyclopentenones that differ from OPDA in the number of carbons, the number of double bonds, or both (Fig. 1*A* and *SI Appendix*, Extended Data Fig. 1). Interestingly, we found a wound-inducible peak (*m*/*z* [mass over charge] = 315.1966) that suggested the presence of an OPDA-like molecule that could originate from EPA (Fig. 1*B*). Content of this molecule peaked around 30 min after wounding and remained elevated at all time points tested (Fig. 1*C*). To confirm the existence of such a molecule, we incubated *Marchantia* whole extracts with EPA or AA as a control. Incubations of *Marchantia* extracts with AA produced an enriched peak (peak 3 in *SI Appendix*, Extended Data Fig. 2*A*) with a retention time (r.t.) of 17.00 min and an *m*/*z* of 422.4 (molecular ion) in the gas chromatography – mass spectrometry chromatogram; this peak was identified as the α-ketol (methyl ester and trimethylsilyl derivatized) produced by the sequential action of a 15-LOX and AOS on AA. However, no OPDA-like compound was detected. On the contrary, upon EPA incubation, a peak with an r.t. of 16.40 min (peak 4 in *SI Appendix*, Extended Data Fig. 2*B*) and an *m*/*z* of 330.2 (methyl ester derivative) indicated the presence, along with the corresponding α-ketol (peak 3 in *SI Appendix*, Extended Data Fig. 2*B*), of an OPDA-like molecule that we termed C20-OPDA. C20-OPDA possesses two more carbons than OPDA on its carboxyl-containing side chain and has two additional double bonds at the Δ^5- and Δ^8-positions (Fig. 1*B*). The structure of C20-OPDA was confirmed by comparison (HPLC-HRMS, both full scan and product ion) (*SI Appendix*, Extended Data Fig. 3) with an original synthetic standard (38). Taken together, these data demonstrate the occurrence of an OPDA-like molecule derived from the n3 LCPUFA, EPA (20:5n3).

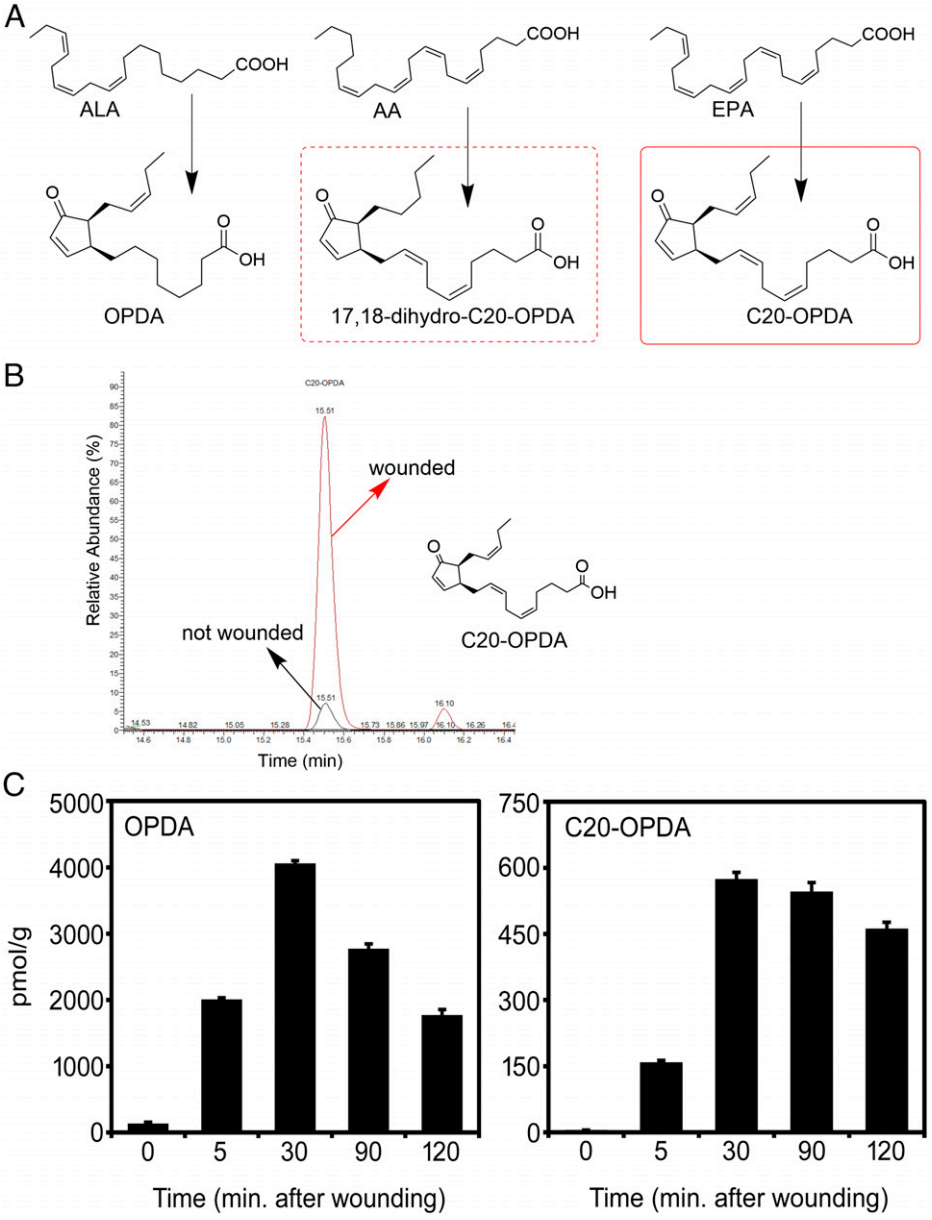

Fig. 1. (*A*) Structure of potential OPDA-like jasmonates that could derive from major PUFAs and LCPUFAs found in *Marchantia*: ALA, AA, and EPA. Hypothesized compounds are squared in red. Dashed lines indicate that the compound was not found under our experimental conditions. (*B*) EIC (extracted ion chromatogram) for *m/z* = 315.1965 (full scan, negative mode, sample of *Marchantia* WT plants under mock conditions [black line] and 30 min after wounding [red line]), which may correspond to the OPDA-like molecule C20-OPDA. (*C*) Accumulation of *cis*-OPDA and C20-OPDA in WT (Tak-1) *Marchantia* plants at indicated time points after mechanical wounding. The experiment was repeated three times with similar results. Error bars represent SEM (n = 3 independent samples, each containing a pool of 12 plants).

C20-OPDA Activates COI1-Dependent and -Independent Jasmonate Responses. As C20-OPDA accumulates in a wound-responsive manner (Fig. 1 *B* and *C*), it may be involved in jasmonate signaling. Growth inhibition is a well-established effect of exogenous jasmonate treatment on plants and has been shown to be largely dependent on the COI1 receptor (3, 10, 39). Thus, we analyzed the growth of WT and Mp*coi1* plants in media containing increasing concentrations of OPDA or C20-OPDA (Fig. 2 *A* and *B*). WT plants responded to increasing concentrations of C20-OPDA similarly to OPDA, with C20-OPDA even displaying a tendency toward being a slightly more potent growth inhibitor (Fig. 2*A*). As expected, Mp*coi1* mutants were largely insensitive to OPDA treatments. Similar to OPDA, low concentrations of C20-OPDA showed limited effects on Mp*coi1* mutants, demonstrating that the growth inhibitory effect of C20-OPDA acts through COI1. At higher tested concentrations, C20-OPDA promoted greater growth inhibition than OPDA in Mp*coi1* (Fig. 2*B*).

In addition to observing its effects in COI1-dependent processes, we also tested the ability of C20-OPDA to activate COI1-independent responses using thermotolerance assays. OPDA and dn-*cis*-OPDA have been shown to protect both WT and Mp*coi1* mutant *Marchantia* plants against heat stress through their electrophilic properties (15). We observed the same effect when plants were exogenously treated with C20-OPDA (Fig. 2 *C* and *D*), confirming that C20-OPDA regulates jasmonate responses both dependent and independent of the COI1 receptor.

To examine the extent to which C20-OPDA– and OPDA-induced responses overlap, we utilized microarrays to obtain transcriptomic profiles of C20-OPDA– or mock-treated WT and Mp*coi1* plants and compared these data with existing microarray analyses on COI1-dependent and -independent OPDA-responsive genes (Fig. 2*E*) (10). In both WT and Mp*coi1* mutant plants, C20-OPDA–regulated genes largely followed a similar pattern to those responsive to OPDA, demonstrating that C20-OPDA activates both COI1-dependent and -independent branches of the jasmonate pathway (Fig. 2*E*, compare columns 1 and 2 [for WT] and columns 3 and 4 [for Mp*coi1*]). Collectively, these data demonstrate that C20-OPDA regulates similar responses to OPDA.

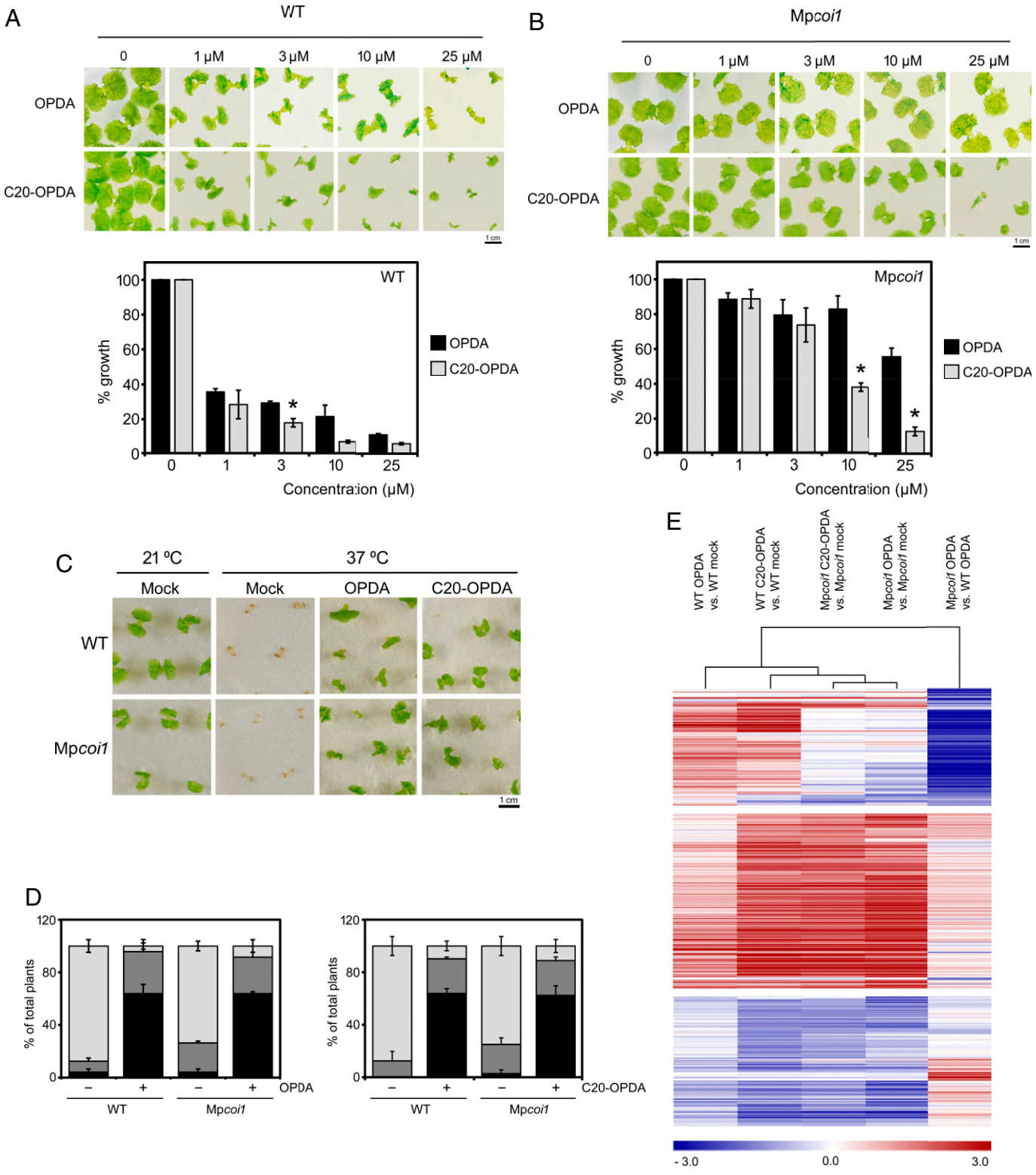

Fig. 2. Effect of increasing concentrations of OPDA and C20-OPDA on the growth of WT (Tak-1; *A*) and Mp*coi1-2* (*B*) plants. Error bars represent SEM ($n = 18$ plants). *Statistically significant differences between percentage growth in OPDA- and C20-OPDA–treated plants at the indicated concentrations (Student's *t* test, $P < 0.05$). (*C*) Effect of 2 h of heat stress at 37 °C on plant survival of WT (Tak-1) and Mp*coi1-2* gemmalings pretreated or not with OPDA or C20-OPDA (25 μM). The experiment was repeated three times with similar results ($n = 24$ plants). (*D*) Quantification of plant phenotypes shown in *C*. Each phenotype (alive, delayed, dead) is represented as a percentage of the total number of plants per experiment ($n = 24$ plants). The experiment was repeated three times. Error bars represent SEM ($n = 3$). (*E*) Analysis of microarray data by hierarchical clustering of differentially expressed [evaluated by the nonparametric algorithm "Rank Product"] genes in response to 2 h of exogenous treatment with mock, OPDA, or C20-OPDA (25 μM) in indicated genotypes. Microarrays were performed after C20-OPDA treatment in WT (WT C20-OPDA vs. WT mock; log ratio > 1/< −1; FDR < 0.001) and Mp*coi1* mutant plants (Mp*coi1* C20-OPDA vs. Mp*coi1* mock; log ratio > 1/< −1; FDR < 0.005), and differentially expressed genes, up- or down-regulated, were compared with available microarray data for the same genes after OPDA treatment in WT or Mp*coi1* plants (WT OPDA vs. WT mock and Mp*coi1* OPDA vs. Mp*coi1* mock) or in the Mp*coi1* mutant compared with WT [Mpcoi1 OPDA vs. WT OPDA (10)]. The analysis is organized into three clusters. Clusters in *Top* and *Middle* represent genes up-regulated after oxylipin treatment (*Top*; COI1-dependent genes; *Middle*, COI1-independent genes), and the cluster in *Bottom* represents down-regulated genes. The total number of genes equals 171; $n = 4$ independent biological replicates formed from six different plants. Hierarchical clustering used Pearson correlation and average linkage.

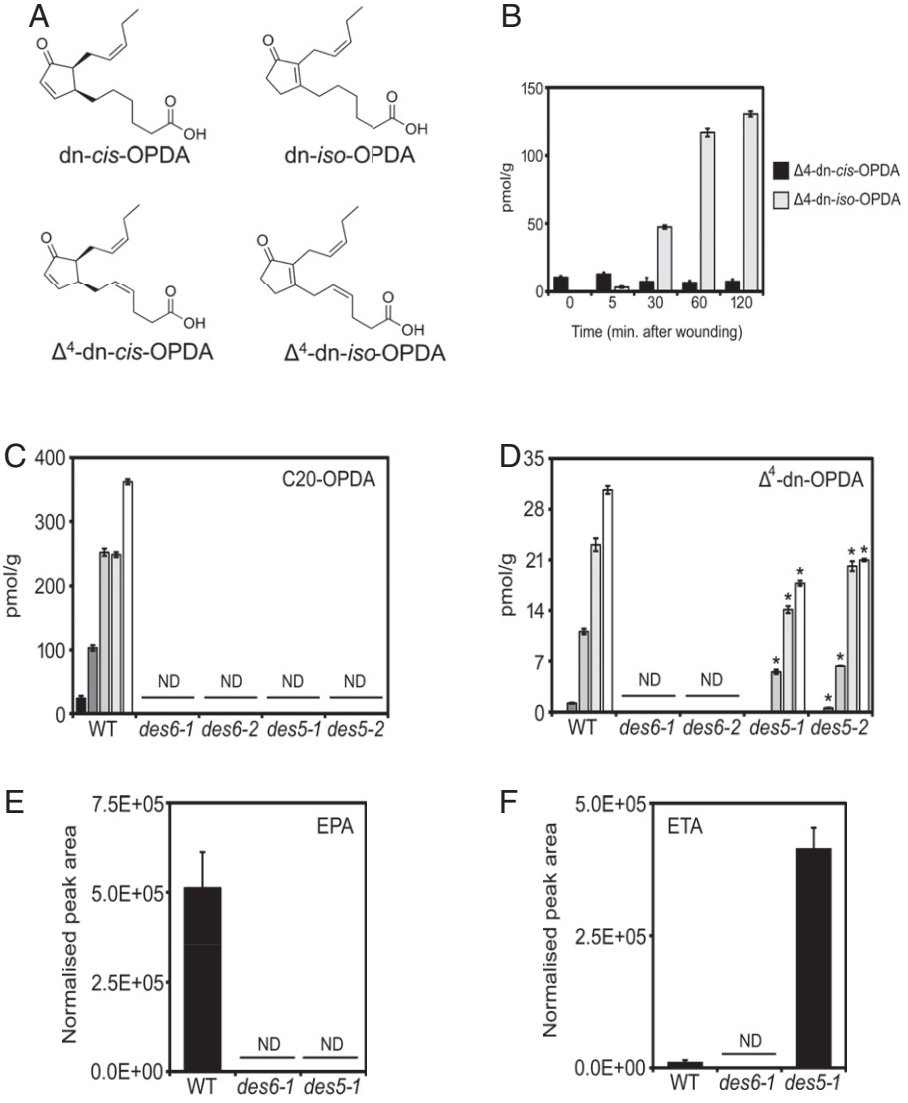

Fig. 3. (*A*) Chemical structures of dn-*cis*-OPDA, dn-*iso*-OPDA, Δ^4-dn-*cis*-OPDA, and Δ^4-dn-*iso*-OPDA. (*B*) Accumulation of Δ^4-dn-OPDA isomers in WT (Tak-1) *Marchantia* plants at indicated time points after mechanical wounding. The experiment was repeated three times with similar results. Error bars represent SEM (n = 3 independent samples, each containing 12 plants). (*C* and *D*) Accumulation of C20-OPDA (*C*) and Δ^4-dn-OPDA (*D*) in WT (Tak-1), Mp*des6-1*, Mp*des6-2*, Mp*des5-1*, and Mp*des5-2* plants at indicated time points after mechanical wounding. The experiment was repeated three times with similar results. Error bars represent SEM (n = 3 independent samples, each containing six plants). Tukey's HSD (honestly significant difference) ANOVA tests were performed to determine statistically significant differences between the five genotypes at any given time point (α = 0.05, n = 3), and asterisks are used to indicate where a sample differs significantly from WT at the same time point. (*E* and *F*) Measurements of LCPUFAs, EPA (*E*), and ETA (*F*) in WT (Tak-1), *des6-1*, and *des5-1 Marchantia* plants. Error bars represent SD of the mean (n = 3 independent samples, each containing six plants). ND denotes that the molecule was not detected.

C20-OPDA Gives Rise to a dn-ODPA–Like Molecule, Δ^4-dn-OPDA. A previous study in *Marchantia* showed that although exogenous OPDA treatment of plants triggers jasmonate responses, OPDA itself cannot bind the MpCOI1 receptor (10). Instead, two dn-OPDA isomers, dn-*cis*-OPDA and dn-*iso*-OPDA, act as MpCOI1 ligands activating jasmonate signaling (Fig. 3*A*) (10). Given the structural differences between C20-OPDA and dn-OPDA (Figs. 1*B* and 3*A*, respectively), we hypothesized that C20-OPDA would not be able to bind the COI1 receptor directly. Indeed, a pull-down assay between plants overexpressing MpCOI1 and recombinant MpJAZ confirmed that C20-OPDA was unable to induce coreceptor interaction (*SI Appendix*, Extended Data Fig. 9*E*). Thus, we supposed that C20-OPDA could be the precursor of a dn-OPDA–like molecule (Fig. 3*A*) (Δ^4-dn-*cis*-OPDA and -*iso*-OPDA), which may act as an additional MpCOI1 ligand. We then mined samples of wounded WT *Marchantia* in order to identify a C16 dn-OPDA–like molecule that could be produced from C20-OPDA after two rounds of β-oxidation. Indeed, we found two peaks that matched the exact mass (m/z = 261.1496) of such a molecule in the extracted ion chromatograms of wounded *Marchantia* samples. One of the peaks (r.t. of 12.98 min) was clearly wound inducible, while the other peak (r.t. = 13.13 min) remained largely unchanged upon wounding (Fig. 3*B* and *SI Appendix*, Extended Data Fig. 4*A*). These data are consistent with what is observed in the case of dn-OPDA, which exists as two positional isomers, namely dn-*cis*-OPDA and dn-*iso*-OPDA (Fig. 3*A* and *SI Appendix*, Extended Data Fig. 5*A*). We named the molecule Δ^4-dn-OPDA. Δ^4-dn-OPDA possesses the same number of carbon atoms as dn-OPDA but with an additional double bond at the fourth carbon (Δ^4) position (Fig. 3*A*). To unambiguously establish the existence of Δ^4-dn-OPDA, we attempted the chemical synthesis of standards for both isomers, Δ^4-dn-*cis*-OPDA and Δ^4-dn-*iso*-OPDA. While the chemical synthesis of the *cis* isomer was straightforward (*SI Appendix*, *SI Text*), we were unable to synthesize the *iso* form; instead of Δ^4-dn-*iso*-OPDA, we obtained Δ^5-dn-*iso*-OPDA. Most likely, the double-bond migration from the Δ^4- to the Δ^5-position occurred to form a more stable *trans* and conjugated double bond, with the double bond in the cyclopentenone ring (*SI Appendix*, Extended Data Fig. 4*B* and *SI Text*). Nonetheless, we were able to employ the synthetic standards in a series of HPLC-HRMS experiments to establish first that the peak with r.t. of 13.13 min corresponds to Δ^4-dn-*cis*-OPDA (full coincidence of r.t. and fragmentation pattern with the synthetic original standard) and second, that the wound-inducible peak that elutes earlier is the *iso* form of this molecule (i.e., Δ^4-dn-*iso*-OPDA) (*SI Appendix*, Fig. S1; *SI Appendix*, *SI Text* has a detailed structure elucidation). Given the difficulty of synthesizing Δ^4-dn-*iso*-OPDA, the larger availability of synthetic Δ^4-dn-*cis*-OPDA, and the proven functional equivalence between the *cis* and *iso* forms of the canonical hormone dn-OPDA (10, 11), hereafter, we

employ Δ^4-dn-*cis*-OPDA in exogenous treatments. However, endogenous measurements of Δ^4-dn-OPDA from plants refer to the sum of both isomers. To confirm C20-OPDA as a direct source of Δ^4-dn-OPDA, we treated WT *Marchantia* plants with C20-OPDA and measured the accumulation of both molecules. Exogenous treatment with C20-OPDA produced a strong burst of Δ^4-dn-OPDA (*SI Appendix*, Extended Data Fig. 5*B*), thus supporting that Δ^4-dn-OPDA is derived from C20-OPDA and accumulates upon wounding (Fig. 3*B*).

The LCPUFA EPA Is a Major Source of Δ^4-dn-OPDA in *Marchantia*. Next, we further explored the biosynthetic pathway of Δ^4-dn-OPDA. Since C20-OPDA was shown to accumulate in *Marchantia* crude extract upon treatment with EPA (*SI Appendix*, Extended Data Fig. 2*B*), we propose that biosynthesis of Δ^4-dn-OPDA occurs via the n3 pathway of LCPFUAs. The components of the n3 pathway are well characterized in *Marchantia*; ALA is converted to EPA in a series of reactions catalyzed by Δ^6-desaturase (MpDES6), Δ^6-elongase (MpELO1), and Δ^5-desaturase (MpDES5) enzymes (*SI Appendix*, Extended Data Fig. 1) (27, 40). Thus, we first created mutants of Mp*DES5* and Mp*DES6* genes using CRISPR-Cas9 technology (*SI Appendix*, Extended Data Fig. 6) (41, 42). We measured PUFA and jasmonate content in Mp*des6* and Mp*des5* mutants to explore the origins of C20-OPDA and Δ^4-dn-OPDA (Fig. 3 *C*–*F*). Consistent with our prediction, neither Mp*des6* nor Mp*des5* plants accumulated C20-OPDA after wounding (Fig. 3*C*), which can be explained by their inability to produce EPA (Fig. 3*E*). Surprisingly, while no Δ^4-dn-OPDA was found in Mp*des6* mutant plants, Mp*des5* mutants accumulated this molecule after wounding in a similar pattern to WT plants, albeit at lower quantities (Fig. 3*D*), demonstrating that Δ^4-dn-OPDA can also be produced through an EPA- and C20-OPDA–independent route. MpDES5 converts eicosatetraenoic acid (ETA) into EPA (*SI Appendix*, Extended Data Fig. 7), and so, while Mp*des5* mutants did not accumulate EPA (Fig. 3*E*), they hyperaccumulated ETA (Fig. 3*F*), indicating that ETA could be a direct source of Δ^4-dn-OPDA (*SI Appendix*, Extended Data Fig. 7). However, it cannot be ruled out that Δ^4-dn-OPDA could also be produced directly from stearidonic acid (SDA) via a single round of β-oxidation (*SI Appendix*, Extended Data Fig. 7). Since Mp*des6* mutants produced neither EPA nor ETA (Fig. 3 *E* and *F*) and are not expected to accumulate SDA (*SI Appendix*, Extended Data Fig. 7), they cannot produce any Δ^4-dn-OPDA (Fig. 3*D*). Given that decreased Δ^4-dn-OPDA levels occur in the absence of EPA in Mp*des5* mutants (Fig. 3*D*), despite a vast increase in ETA production (Fig. 3*F*), we propose that EPA is a major source of Δ^4-dn-OPDA in *Marchantia*. While both SDA and ETA could act as alternate direct sources of Δ^4-dn-OPDA, their relative contributions to the overall levels of this hormone remain to be elucidated.

Our measurements showed small decreases in OPDA, dn-*cis*-OPDA, and dn-*iso*-OPDA in Mp*des6*, which were slightly more pronounced in Mp*des5* mutants (*SI Appendix*, Extended Data Fig. 8). These differences likely reflect the effects of disrupting the natural equilibrium of the FA profile of the plant, including molecules from the n6 pathway, which are also expected to be affected in Mp*des5* and Mp*des6* mutants (*SI Appendix*, Extended Data Fig. 7). Overall, our results indicate that Δ^4-dn-OPDA is synthesized in the n3 biosynthetic pathway of LCPUFAs, primarily from EPA-derived C20-OPDA.

Δ^4-dn-OPDA Is a Ligand of MpCOI1. Given the structural homology between Δ^4-dn-OPDA and dn-OPDA and that like dn-OPDA, Δ^4-dn-OPDA is wound responsive (Fig. 3*B* and *SI Appendix*, Extended Data Fig. 5*A*), we hypothesized that Δ^4-dn-OPDA may be a ligand of the jasmonate coreceptor complex (MpCOI1–MpJAZ) and have a role in signal transduction. To assess the effect of Δ^4-dn-OPDA on jasmonate-regulated processes, we analyzed its growth inhibition effects compared with OPDA and dn-*iso*-OPDA (Fig. 4 *A* and *B*). dn-*iso*-OPDA was used for comparison because it was previously shown to interact more strongly in pull-down assays than dn-*cis*-OPDA (10). Δ^4-dn-*cis*-OPDA behaved as OPDA and dn-*iso*-OPDA, inhibiting the growth of WT plants, and like dn-*iso*-OPDA, it was seen to be a more potent growth inhibitor than OPDA at 50 μM treatments (Fig. 4*A*). Mp*coi1* mutants were much less sensitive to these molecules than WT plants, although both dn-*iso*-OPDA and Δ^4-dn-OPDA showed a stronger growth inhibitory effect than OPDA at higher tested concentrations (Fig. 4*B*). Next, we performed qPCR analysis of known JRG in WT and Mp*coi1* plants treated with Δ^4-dn-*cis*-OPDA or dn-*cis*-OPDA or mock treated. In this case, dn-*cis*-OPDA was used as a positive control since unlike dn-*iso*-OPDA, it activates both COI1-dependent and -independent genes (15). Consistent with the overlapping gene expression patterns of C20-OPDA and OPDA (Fig. 2*E*), our data suggest that Δ^4-dn-*cis*-OPDA activates the same set of JRG as dn-*cis*-OPDA and acts on both COI1-dependent and -independent genes (*SI Appendix*, Extended Data Fig. 9 *A*–*D*).

Both dn-OPDA isomers have been demonstrated to bind the MpCOI1 receptor and trigger its interaction with the MpJAZ repressor (10). To determine if Δ^4-dn-OPDA is a ligand of MpCOI1, we performed pull-down assays between Flag-tagged MpCOI1 expressed in planta and recombinant MpJAZ protein (Fig. 4*C*). Since dn-*iso*-OPDA triggers stronger coreceptor interaction than its *cis* counterpart (10), we used dn-*iso*-OPDA as a positive control and OPDA, which does not promote MpCOI1–MpJAZ interaction, as a negative control. As expected, we did not identify MpCOI1 in OPDA-treated samples but observed increasing levels of MpCOI1 retention by MBP–MpJAZ correlated to greater concentrations of dn-*iso*-OPDA. Importantly, we observed that the addition of Δ^4-dn-*cis*-OPDA was able to facilitate MpCOI1–MpJAZ interaction even more strongly than dn-*iso*-OPDA (Fig. 4*C*). Although it was not possible to synthesize Δ^4-dn-*iso*-OPDA, we demonstrated that Δ^5-dn-*iso*-OPDA, a compound structurally similar to Δ^4-dn-*iso*-OPDA, was able to induce MpCOI1–MpJAZ interaction (*SI Appendix*, Extended Data Fig. 9*E*). Taken together, our data indicate that Δ^4-dn-OPDA is a bona fide bioactive hormone, capable of activating jasmonate-dependent responses.

Both Δ^4-dn-OPDA and dn-OPDA Are Required to Fully Activate Jasmonate Responses. We next sought to investigate the role of endogenous Δ^4-dn-OPDA in jasmonate signaling. Recent findings have demonstrated that the main source of dn-OPDA in *Marchantia* is HTA (16:3n3), and as such, the Mp*fad5* mutant (MpFAD5 specifically synthesizes HTA) is impaired in dn-OPDA accumulation, with an almost complete absence of the *cis* form and vast reduction of the *iso* form (24). Consequently, it was somewhat surprising that Mp*fad5* mutants did not appear substantially affected in jasmonate-dependent responses (24). Now, considering the identification of Δ^4-dn-OPDA as a bioactive ligand of MpCOI1, we hypothesized that the weakly compromised jasmonate responses in Mp*fad5* could be explained by the presence of Δ^4-dn-OPDA in this mutant. To test this, we analyzed the accumulation of Δ^4-dn-OPDA in Mp*fad5* mutants and discovered levels comparable with that of the WT (Fig. 5*B*). Since Mp*fad5* mutant plants are largely impaired in dn-OPDA accumulation (Fig. 5 *D* and *E*) (24) and

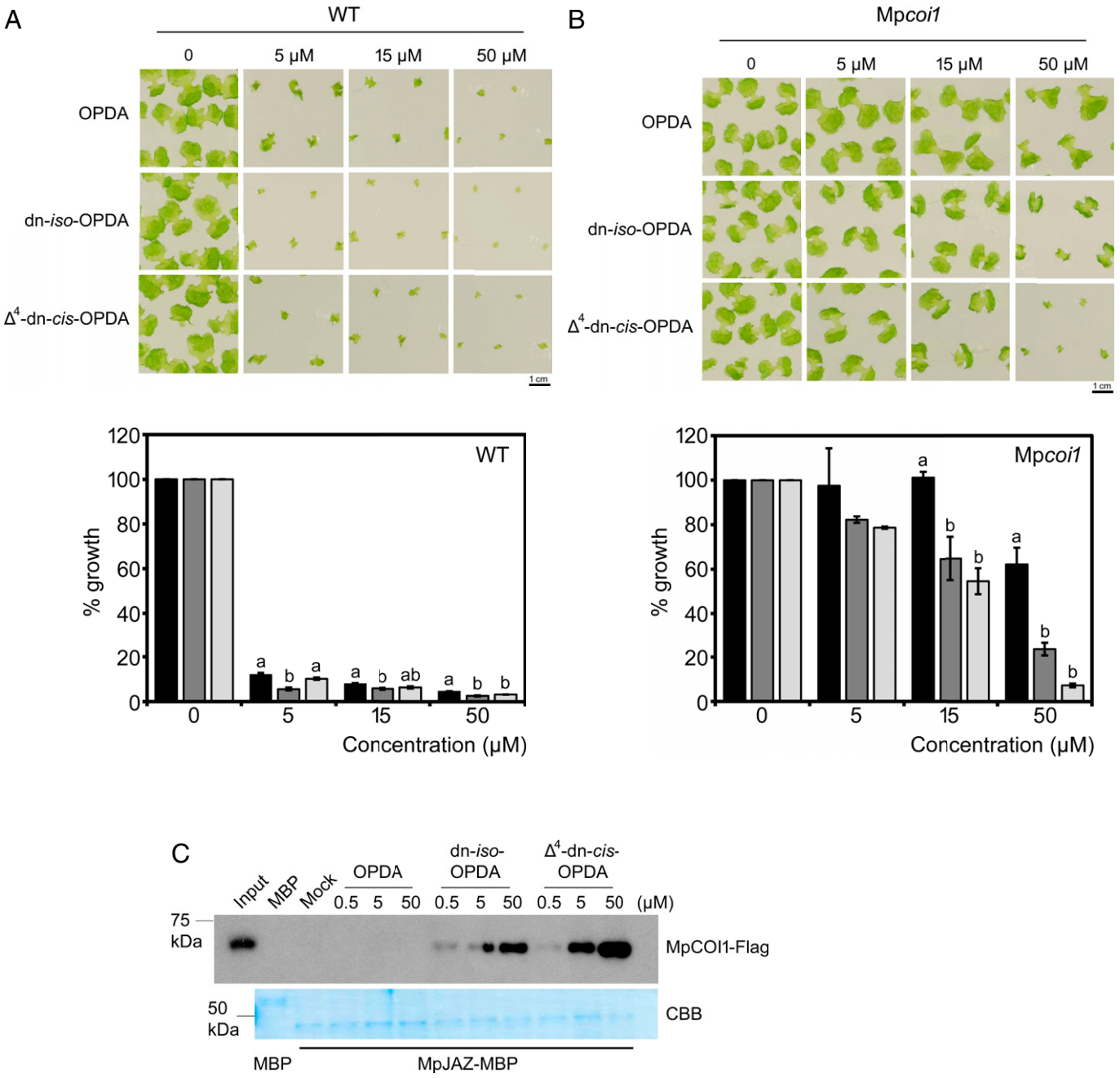

Fig. 4. (*A* and *B*) Effect of increasing concentrations of OPDA, dn-*iso*-OPDA, and Δ[4]-dn-*cis*-OPDA on the growth of WT (Tak-1; *A*) and Mp*coi1-2* (*B*) plants. Error bars represent SEM (n = 18 plants). Different letters indicate statistically significant differences between the percentage of growth in OPDA-, dn-*iso*-OPDA–, and Δ[4]-dn-*cis*-OPDA–treated plants at the indicated concentration (Tukey's HSD [honestly significant difference] ANOVA test; α = 0.05, n = 18). (*C*) 35S:MpCOI1-Flag–expressing *Arabidopsis* plant extracts were incubated with MpJAZ–MBP (maltose binding protein) protein or MBP alone with OPDA, dn-*iso*-OPDA, Δ[4]-dn-*cis*-OPDA, or mock treatment in the pull-down buffer (the indicated concentrations). (*Upper*) Immunoblot with anti-Flag antibody. (*Lower*) Coomassie blue staining of MpJAZ–MBP after cleavage with Factor Xa. The experiment was repeated three times with similar results. CBB, Coomassie Brilliant Blue.

Mp*des6* plants lack Δ[4]-dn-OPDA completely (Figs. 3*D* and 5*B*), we used CRISPR/Cas9 to obtain Mp*des6fad5* double mutants to limit both sets of molecules. (*SI Appendix*, Extended Data Fig. 10). We measured the accumulation of OPDA, C20-OPDA, both isomers of dn-OPDA and Δ[4]-dn-OPDA in the double Mp*des6fad5* mutant, Mp*des6* and Mp*fad5* single mutants, and WT controls (Fig. 5). While OPDA levels were only slightly reduced from WT levels in Mp*des6fad5* plants and very low levels of dn-*iso*-OPDA persisted (produced directly from OPDA), dn-*cis*-OPDA, C20-OPDA, and Δ[4]-dn-OPDA did not accumulate in the double mutant. We, therefore, collected tissue of WT, Mp*coi1*, and Mp*des6fad5* mutant plants 90 min after wounding (or mock conditions) and performed RNA-seq (next-generation sequencing technique) analysis (Fig. 6 *A* and *B*). We specifically looked at wound-responsive genes and found that from a total of 325 COI1-dependent genes that were differentially expressed after wounding (log ratio > |1.5|, false discovery rate [FDR] < 0.05) (Fig. 6*A*, clusters 1 and 2), about 40% were down-regulated in the Mp*des6fad5* double mutants compared with WT plants (Fig. 6*A*, cluster 1). Consistent with the jasmonate profile of the Mp*des6fad5* mutant plants (Fig. 5) and known jasmonate responses, these genes were specifically related to "jasmonate, FA, and oxylipin biosynthesis" and "response to wounding" (Fig. 6*B*). A selection of genes from cluster 1 was confirmed by qPCR, and their expression was compared with that observed in the respective single mutants, with

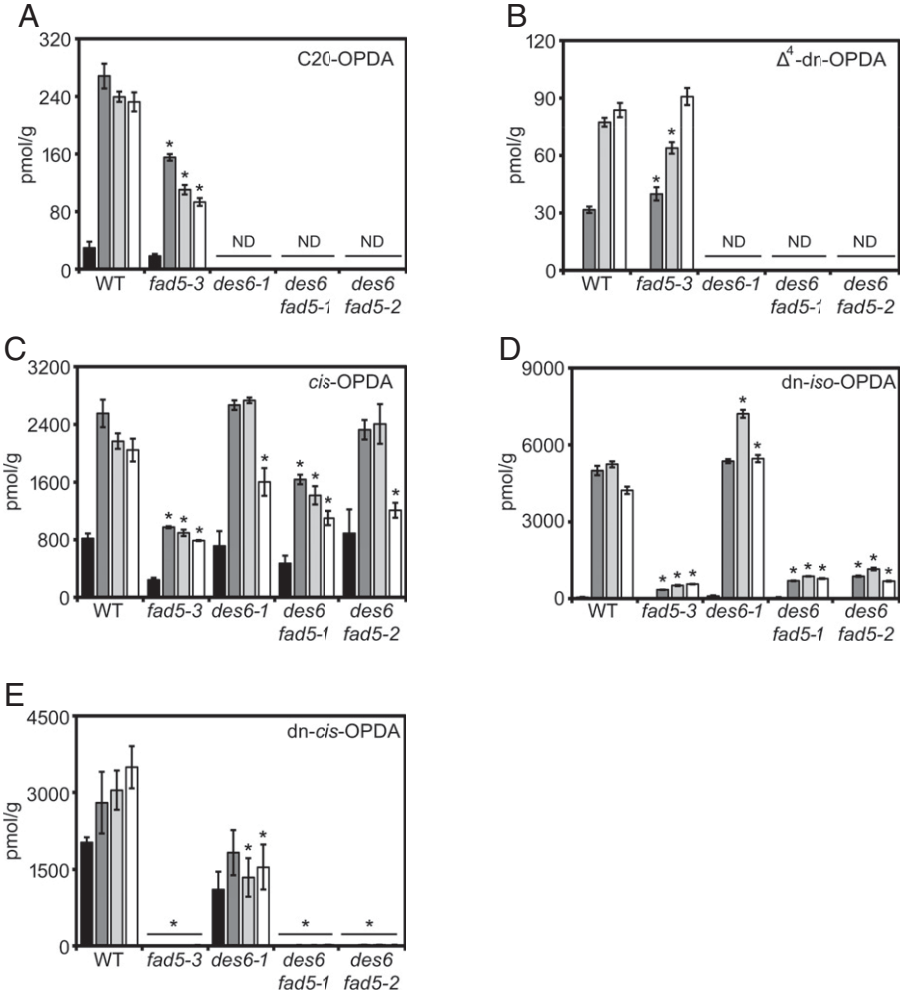

Fig. 5. Accumulation of C20-OPDA (*A*), Δ^4-dn-OPDA (*B*), *cis*-OPDA (*C*), dn-*iso*-OPDA (*D*), and dn-*cis*-OPDA (*E*) in WT (Tak-1), Mp*fad5-3*, Mp*des6-1*, Mp*des6fad5-1*, and Mp*des6fad5-2* plants at indicated time points after mechanical wounding. Error bars represent SEM ($n = 3$ independent samples, each containing six plants). Tukey's HSD (honestly significant difference) ANOVA tests were performed to determine statistically significant differences between the five genotypes at any given time point ($\alpha = 0.05$, $n = 3$), and asterisks are used to indicate where a sample differs significantly from WT at the same time point. ND, not detected.

and without wounding (Fig. 6 *C–F*). For all genes tested, we observed that knocking out *FAD5* or *DES6* alone produced little or no reduction in gene expression (and in some cases, an increase compared with WT), but significant decreases comparable with expression in Mp*coi1* were seen in the double Mp*des6-fad5* mutant plants. In addition to these affected wound up-regulated genes, several genes that were down-regulated during wounding in WT plants were not down-regulated in the double mutant, similarly to Mp*coi1* (Fig. 6*A*, cluster 4). Interestingly, a subset of COI1-independent genes was seen to be up-regulated in the Mp*des6fad5* mutant (Fig. 6*A*, cluster 3). These genes are likely a result of the electrophilic effects of OPDA (14, 15), for which levels remain high in the double mutant (Fig. 5*C*). Despite a large proportion of wound-inducible genes being down-regulated in the Mp*fad5des6* double mutant, there was also a significant portion that was unaffected (Fig. 6*A*, cluster 2). This may be indicative of further as of yet undiscovered bioactive molecules that are involved in the wound-induced signaling pathway, such as those derived from the n6 biosynthetic pathway (43, 44), but most likely, it highlights the significance of the small quantity of OPDA-derived dn-*iso*-OPDA that accumulates in these plants. Overall, our transcriptomic analyses indicate that both dn-OPDA and Δ^4-dn-OPDA are required for a complete activation of JRG in *Marchantia*.

To examine the biological relevance of the altered gene expression profile of Mp*des6fad5* mutants in comparison with WT and the respective single mutants (Fig. 6 *A–F*) (24), we studied well-known jasmonate-mediated defense responses: those against herbivory and fungal pathogen infections. In the herbivory assays, larvae of the beet armyworm (*Spodoptera exigua*; Lepidoptera) were allowed to feed on thalli of 6-wk-old WT, Mp*coi1*, Mp*fad5*, Mp*des6*, and Mp*des6fad5* plants, and their performance (larval weight) was analyzed after 7 d. As previously found, we observed significantly higher larval weight in larvae fed on Mp*coi1* plants than on WT and Mp*fad5* single mutants due to the compromised defense response of Mp*coi1* mutants against insect attack (Fig. 6*G*) (10, 24). Larvae from Mp*des6* plants were slightly larger than those from WT and Mp*fad5*. Remarkably, larvae fed on Mp*des6fad5* double-mutant plants were significantly larger than those fed on WT and the Mp*fad5* mutant alone, almost to the level of the Mp*coi1* mutants (Fig. 6*G*). These data indicate that the double Mp*des6fad5* mutant plants were more susceptible to insect feeding than the WT plants or the respective single mutants. Next, we studied the response of the same set of plants to the hemibiotrophic fungus *Fusarium oxysporum* (*Fo*), for which a pathosystem with *Marchantia* has recently been established (45). Defense responses against hemibiotrophic pathogens, such as *Pseudomonas syringae*, are mediated by the phytohormone salicylic acid (SA). In defense responses, jasmonate and SA signaling have generally been shown to be antagonistic to one another, and thus, activation of the jasmonate pathway with the aim of lowering SA defenses has evolved as a key mechanism employed by pathogens (46). Indeed, in the case of *Fo*, it has previously been observed in *Arabidopsis* that an inability by the plant to perceive JA is correlated with an increase in

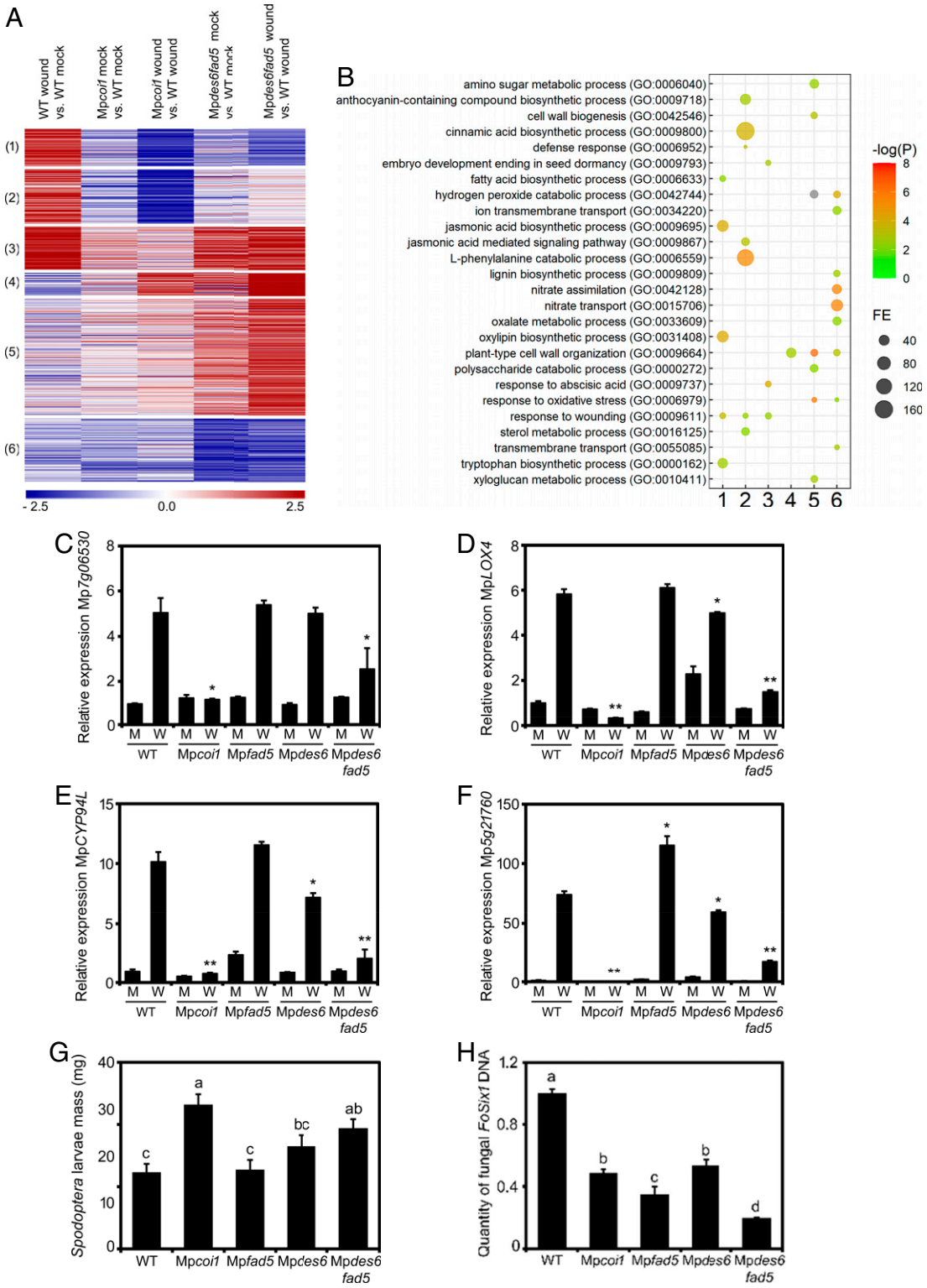

Fig. 6. (*A*) Analysis of RNA-seq data by K-means clustering of genes differentially expressed [evaluated by EdgeR (68)] in response to mechanical wounding (90 min) in the genotypes indicated (log ratio > 1.5/< −1.5; FDR < 0.05). Six clusters were generated and grouped for gene ontology (GO) analysis. (*B*) Significant GO terms (biological process) associated with each of the clusters indicated in *A*. GO terms correspond to the most similar genes in *Arabidopsis*. FE, fold enrichment of the term in the cluster. (*C*–*F*) Analysis by qPCR of wound-responsive genes in WT (Tak-1), Mp*coi1-2*, Mp*fad5-3*, Mp*des6-1*, Mp*des6fad5-1*, and Mp*des6fad5-2 Marchantia* plants under mock conditions or 90 min after mechanical wounding. Expression of genes coding for an aromatic L-amino acid/L-tryptophan decarboxylase (Mp*7g06530*), LOX4 (Mp*LOX4*; Mp*5g21680*), Cytochrome P450 CYP94 like (Mp*CYP94L*; Mp*2g10330*), and a Patatin-like phospholipase (Mp*5g21760*) was normalized against Mp*APT* (Mp*3g25140*). Error bars represent SD (n = 3). Asterisks represent statistically significant differences between the indicated sample and WT after wounding (Student's t test). *P < 0.05; **P < 0.005. M (mock conditions), W (90 min after mechanical wounding). (*G*) Larval weight of *S. exigua* after 7 d feeding on thalli of WT (Tak-1), Mp*coi1*-2, Mp*fad5-3*, Mp*des6-1*, and Mp*des6fad5-1* plants. Error bars represent SEM (n = 24 plants). Different letters indicate statistically significant differences between the five genotypes tested (Tukey's HSD ANOVA test; α = 0.05). The experiment was repeated three times with similar results obtained. (*H*) Quantification by qPCR of *Fo* gene *Six1* in DNA obtained from thallus of WT (Tak-1), Mp*coi1*-2, Mp*fad5-3*, Mp*des6-1*, and Mp*des6fad5-1* plants 2 d after dip inoculation with *Fo* (10^6 spores mL^{-1}). DNA levels were normalized against Mp*EF1α*. Error bars indicate SD (n = 3). Different letters indicate statistically significant differences between the five genotypes tested (Tukey's HSD [honestly significant difference] ANOVA test; α = 0.05). The experiment was repeated three times with similar results.

resistance to *Fo*. Thus, we hypothesized that biosynthetic mutants of dn-OPDA and Δ^4-dn-OPDA may exhibit increased resistance to *Fo*. Plants were treated with *Fo* by dip inoculation (10^6 spores mL^{-1}), and fungal DNA isolated from thallus tissue was quantified 2 d postinfection (Fig. 6*H* and *SI Appendix*, Extended Data Fig. 10*B*). Consistent with previous reports on the role of jasmonates in hemibiotrophic pathogen infection (47), Mp*coi1* plants were found to be more resistant to *Fo* than WT. Interestingly, both Mp*fad5* and Mp*des6* single mutants displayed resistance comparable with or greater than Mp*coi1*, indicating that plant-produced jasmonates are crucial to *Fo* activity in *Marchantia*. Remarkably, fungal DNA levels taken from Mp*des6fad5* double-mutant plants were significantly lower than both single mutants alone (Fig. 6*H*), indicating that the effects of removing dn-OPDA and Δ^4-dn-OPDA on plant defenses against *Fo* are additive.

Together, these data suggest that both dn-OPDA and Δ^4-dn-OPDA contribute to jasmonate-regulated defense responses in *Marchantia*.

Discussion

For decades, vascular plant model systems, such as *A. thaliana* and *Solanum lycopersicum*, have dominated studies on the jasmonate signaling pathway. However, in recent years, work in a variety of nonvascular plant species has begun to elucidate novel components of jasmonate signaling and shed light on the evolutionary history of the pathway (48). A breakthrough finding was the discovery that the bioactive jasmonate in vascular plants, JA-Ile, is not shared in the model bryophyte, *Marchantia*, which instead utilizes the JA-Ile precursor, dn-OPDA, as the hormone (10). dn-OPDA and JA-Ile are produced from C16 and C18 PUFAs, which are found ubiquitously across the plant kingdom (16, 49). However, LCPUFAs can also be found in algae, bryophytes, and some lycophytes but are not commonly found in angiosperms (50, 51). LCPUFAs, such as AA and EPA, are also present in fungi, bacteria, and animals. Indeed, due to their beneficial role in human health and potential as a source of biofuel production, a comprehensive understanding of the biosynthetic pathways of these molecules is available in the scientific literature (30). However, since molecular studies on signaling pathways have largely been confined to vascular plants, the downstream products of these LCPUFAs and their role in signal transduction have remained vastly understudied. Here, we report the identification of a dn-OPDA–like molecule derived from LCPUFAs (primarily EPA, via C20-OPDA), which we name Δ^4-dn-OPDA (Figs. 1 and 3). We demonstrate Δ^4-dn-OPDA to be a ligand of MpCOI1, an essential component in the plant's response to wounding and insect attack and important in producing a WT response during fungal pathogen infection (Figs. 4*C* and 6).

The potential for the existence of novel bioactive jasmonates working alongside dn-OPDA was recently highlighted in a study in *Marchantia*. It was found that Mp*fad5* mutant plants, which accumulate negligible levels of dn-*cis*-OPDA and just 5 to 10% of the WT level of dn-*iso*-OPDA, had only minor disturbances in the transcriptomic response to wounding and were able to defend against insects as well as WT plants in herbivory assays (24). Two main possibilities were proposed to explain these findings: first, that the small amount of dn-*iso*-OPDA in the plant, presumed to form directly from OPDA, was sufficient to activate the majority of the JRGs and provide a robust defense against insect feeding and second, that dn-OPDA was not the only MpCOI1 ligand capable of activating jasmonate responses (24). The discovery of Δ^4-dn-OPDA and the data presented in this paper demonstrate that both explanations merit some credit.

We show that LCPUFA-derived Δ^4-dn-OPDA is a bona fide MpCOI1 ligand and that it activates similar responses to dn-OPDA (Figs. 4–6). Furthermore, using mutants of two desaturase enzymes in the biosynthetic pathway of LCPUFAs, Mp*des6* and Mp*des5*, we determine that Δ^4-dn-OPDA is produced in a separate parallel pathway to dn-OPDA (Fig. 3). These two pathways utilize the same set of enzymes, some of which are specific, like the FADs involved, and others are general, such as LOX, AOS, and AOC enzymes (3). It should be noted that in order to be processed by these general enzymes, endoplasmic reticulum (ER)-localized LCPUFAs are predicted to move first to the plastids, as has previously been described for the exchange of metabolites (52). Since Δ^4-dn-OPDA and dn-OPDA originate from independent sources (i.e., different PUFAs or LCPUFAs), the two pathways are independent. As such, the effects of removing one of these pathways are likely to be compensated for by the actions of the other, which may partly explain the unexpected canonical jasmonate-regulated responses seen in the Mp*fad5* single mutant (24). Indeed, when we removed Δ^4-dn-OPDA production in the Mp*fad5* background (using Mp*des6fad5* double mutants), we observed an additive effect on wound-responsive gene expression and defense against herbivory and fungal infection, indicating that both molecules are required for a complete jasmonate response (Fig. 6). Interestingly, while Mp*des6fad5* double mutants were more susceptible to insect feeding than both Mp*fad5* and Mp*des6* single mutants, their difference from Mp*des6* mutant plants was less marked than Mp*fad5* mutants (Fig. 6*G*). This is likely a result of the increased flavonoid content of Mp*fad5* single mutants since flavonoids are known to have antifeedant activity (24, 53). However, it is also possible that some specificity exist between Δ^4-dn-OPDA and dn-OPDA with regard to their role in different jasmonate responses. Indeed, the kinetics of the molecules' accumulation after wounding were seen to be slightly different, with Δ^4-dn-OPDA appearing more slowly than dn-OPDA but continuing to rise at later time points (Fig. 3*B* and *SI Appendix*, Extended Data Fig. 5*A*). Moreover, at the times tested, Δ^4-dn-OPDA concentrations were lower than those of dn-OPDA (Fig. 3*B* and *SI Appendix*, Extended Data Fig. 5*A*). Interestingly, biosynthetic FADs that produce the two molecules reside in different subcellular compartments; Δ^6- and Δ^5-desaturases involved in Δ^4-dn-OPDA production, such as MpDES6 and MpDES5, are found in the ER, whereas the Δ^7-desaturase MpFAD5, which produces the majority of the dn-OPDA in *Marchantia* (24), is plastid localized (29, 54). The endogenous concentrations of Δ^4-dn-OPDA and dn-OPDA, therefore, likely differ between cellular compartments, and this may impact their transportation to the cytoplasm and nucleus, where they interact with COI1. In pull-down assays, Δ^4-dn-OPDA was a stronger ligand than dn-*iso*-OPDA (Fig. 4*C*), although the relevance of this in planta remains to be investigated. One potential explanation for this is the presence of the double bond at the Δ^4-position, which may limit the flexibility of the carboxyl-containing side chain, therefore facilitating the packing of the molecule in the binding pocket of MpCOI1. Further studies are needed to determine the relative contributions of each molecule to specific responses and in different cellular compartments to fully analyze the interplay between the two hormones in activating COI1-medidated signaling.

Despite having a clear contributory role in jasmonate responses alongside dn-OPDA, the existence of Δ^4-dn-OPDA alone is not sufficient to explain the Mp*fad5* phenotype 24. While our results

demonstrated that around 40% of the COI1-dependent wound-inducible genes studied were down-regulated in Mp*des6fad5* double-mutant plants compared with WT (Fig. 6*A*), that still leaves a significant portion of genes that were unaffected, despite the double mutant having only a minor portion of the WT levels of dn-*iso*-OPDA and a complete absence of both dn-*cis*-OPDA and Δ^4-dn-OPDA (Fig. 5). This result indicates that a small quantity of dn-*iso*-OPDA alone may be sufficient to activate a large part of the transcriptomic changes that result from mechanical wounding. It is known that the precursors of bioactive jasmonates, OPDA and JA, accumulate to much higher levels than the corresponding hormones, dn-OPDA and JA-Ile (10, 55, 56). This pattern is also observed here between C20-OPDA and Δ^4-dn-OPDA (Figs. 1*A* and 3*B*). Given this information, it appears that hormone contents are maintained at relatively low levels and that their accumulation is dependent on several factors, such as the perceived stimuli and the particular organelle in which they are produced. In this way, an additional layer of regulation that may aid plant resilience and plasticity can be achieved. While the threshold level of the hormone that is required to activate jasmonate signaling through the COI1 receptor remains unknown, our transcriptomic data suggest that the normal physiological concentrations of bioactive jasmonates may be much higher than the signaling needs of the plant. An additional possibility is that derivatives of dn-OPDA and Δ^4-dn-OPDA (such as the hydroxylated or methylated forms) are accumulating and contributing to jasmonate responses. Indeed, in *Arabidopsis*, it has been shown that the hydroxylated form of JA-Ile, 12-OH-JA-Ile, is a bioactive COI1 ligand, and its absence in cytochrome P450 mutant *b1b3* causes a compromised response to wounding, despite an overaccumulation of JA-Ile (37, 57, 58). Obtaining knowledge on the existence of chemical derivatives of dn-OPDA–like molecules and their contribution to jasmonate signaling is thus an important consideration for future studies. Besides dn-OPDA and Δ^4-dn-OPDA (and their possible derivatives), the potential for other COI1 ligands cannot be ruled out, and further research into the downstream products of PUFAs and LCPUFAs is essential before drawing concrete conclusions on these data. Indeed, it would be interesting to analyze oxylipin levels and jasmonate responses in mutants of enzymes that are general to the biosynthetic pathways of both dn-OPDA and Δ^4-dn-OPDA, such as MpAOC and ω3-FADs, in order to determine the likelihood of such molecules.

The molecules described here represent the identification of LCPUFA-derived jasmonates in green-lineage plants, and thus, the existence of equivalent molecules in other LCPUFA-containing plants should be considered. Furthermore, the significance of these molecules in the evolutionary arms race between plants and pathogens (e.g., fungi), which may also produce LCPUFA-derived oxylipins, presents an interesting question for future studies. The existence of LCPUFAs producing bioactive jasmonates also has potential implications in biotechnology. Given the importance of some LCPUFAs in human health, scientists have begun to investigate the use of transgenic crop plants that ectopically express FAD genes, with the aim of producing plants rich in dietary LCPUFAs (including EPA) (27, 51, 59). That these plants may also (over-)produce downstream signaling jasmonates must be considered to avoid detrimental growth inhibitory effects.

Interestingly, while we were able to identify both *cis* and *iso* forms of Δ^4-dn-OPDA, the *cis* form occurred at extremely low levels, close to the limit of detection. Furthermore, unlike its *iso* counterpart, Δ^4-dn-*cis*-OPDA did not accumulate in response to wounding (Fig. 3*B*). This is somewhat reminiscent of the wound-induced kinetics of dn-OPDA isomers, in which the *cis* isomer is not induced by wounding to the same extent as the *iso* form and is generally found at lower concentrations (Fig. 5 and *SI Appendix*, Extended Data Fig. 8). Due to the reactive nature of the double-bond position in the cyclopentenone rings of dn-*cis*-OPDA and *cis*-OPDA, these molecules have a specific role in electrophilic signaling (13, 15). Despite being utilized in this way, because of their high reactivity, electrophilic molecules may also cause cell damage. Indeed, it has been shown that in some insects, *cis*-OPDA is rapidly converted into the more stable and less reactive *iso* counterpart to avoid the toxicity conferred by the electrophilic character of the *cis* form (60, 61). In plants, jasmonates from C16 and C18 PUFAs, such as dn-*cis*-OPDA and *cis*-OPDA, are formed in the chloroplast, which as a result of its role in photosynthesis, hosts an abundance of detoxification enzymes that help to buffer the reactive nature of these molecules (62, 63). Oxylipins derived from LCPUFAs likely originate in the ER, which is similarly prepared for oxidative stress linked to the process of oxidative protein folding (64). Jasmonate hormones, however, must act in the cytoplasm and nucleus, areas of the cell that may be more susceptible to the damaging effects of electrophilic groups (62). It is possible, therefore, that electrophilic oxylipins, such as dn-*cis*-OPDA and Δ^4-dn-*cis*-OPDA, do not accumulate in response to wounding in the same way as their *iso* forms due to their reactive nature. The accumulation patterns of Δ^4-dn-OPDA thus reinforce the idea that *cis* and *iso* forms of dn-OPDA–like molecules have distinct specialized functions as well as overlapping ones.

In this study, using the nonvascular model plant *M. polymorpha*, we have identified bioactive jasmonates that are derived from LCPUFAs: C20-OPDA and Δ^4-dn-OPDA. Furthermore, we have demonstrated that Δ^4-dn-OPDA is a ligand of the MpCOI1 receptor and shown that both Δ^4-dn-OPDA and the previously identified dn-OPDA are required for full jasmonate response activation. The data presented here highlight the need to look beyond classical plant model systems to uncover unidentified branches of known phytohormone pathways and piece together their evolutionary histories.

Materials and Methods

Materials and methods, including those for chemical and enzymatic synthesis, are described in Supplementary Information file.

Data, Materials, and Software Availability. RNA-seq and microarray data have been deposited in the Gene Expression Omnibus (accession nos. GSE195837 and GSE195838) (65, 66). All other data are included in the article and/or supporting information.

ACKNOWLEDGMENTS. CRISPR constructs containing guideRNAs targeting Mp*DES6* and Mp*DES5* genes were provided to us by Prof. K. T. Yamato (Kindai University). S.K. was supported by European Molecular Biology Organization Long-Term Fellowship ALTF 47-2017 and Spanish Ministry for Science and Education Juan de la Cierva Fellowship IJC2018-035580-I. G.S. was supported by a postdoctoral grant funded by Plan propio de la University of La Rioja and V (five in Roman numbers) Plan Riojano de I + D + I (Investigación + Desarrollo + Innovación). The laboratory of J.M.F.-Z. was funded by MINECO/FEDER (Ministry of Education and Science) Grant BIO2017-86651-P. Work in the laboratory of M.U. was financially supported by Japan Society for the Promotion of Science Grants 18KK0162 (to M.U.) and 20H00402 (to M.U.). G.H.J-A. was supported by the Deutsche Forschungsgemeinschaft Individual Research Fellowship JI 241/2-1. This work was funded by Spanish Ministry for Science and Innovation Grant PID2019-107012RB-100 MICINN/FEDER (Ministry of Science and Innovation) (to R.S.).

Author affiliations: [a]Department of Plant Molecular Genetics, Centro Nacional de Biotecnología, Consejo Superior de Investigaciones Científicas, Madrid 28049, Spain; [b]Facultad de Ciencia y Tecnología, Universidad de La Rioja, Logroño (La Rioja) 26006, Spain; [c]Division of Physiological Chemistry II, Department of Medical Biochemistry and Biophysics, Karolinska Institutet, Stockholm, 17177, Sweden; [d]Department of Environmental Biology, Bioma Institute, University of Navarra, Navarra 31008, Spain; [e]Department of Chemistry, Graduate School of Science, Tohoku University, Sendai 980-8578, Japan; and [f]Centre for Metabolomics and Bioanalysis, Department of Chemistry and Biochemistry, Facultad de Farmacia, Universidad San Pablo-CEU, Centro de Estudios Universitarios, Urbanización Montepríncipe, Boadilla del Monte 28660, Spain

Author contributions: S.K., G.H.J.-A., and R.S. designed research; S.K., G.S., I.M., M.H., A.M.Z., J.M.F.-Z., M.F.R.-S., S.M., S.G.-I., and G.H.J.-A. performed research; M.H., N.K., and M.U. contributed new reagents/analytic tools; S.K., G.S., I.M., M.H., A.M.Z., J.M.G.-M., J.M.F.-Z., M.F.R.-S., C.B., S.M., S.G.-I., and G.H.J.-A. analyzed data; J.M.G.-M. supervised hormone measurements; C.B. supervised FA measurements; and S.K., G.H.J.-A., and R.S. wrote the paper.

The authors declare no competing interest.

1. C. Wasternack, I. Feussner, The oxylipin pathways: Biochemistry and function. *Annu. Rev. Plant Biol.* **69**, 363–386 (2018).
2. J. Goossens, P. Fernández-Calvo, F. Schweizer, A. Goossens, Jasmonates: Signal transduction components and their roles in environmental stress responses. *Plant Mol. Biol.* **91**, 673–689 (2016).
3. C. Wasternack, B. Hause, Jasmonates: Biosynthesis, perception, signal transduction and action in plant stress response, growth and development. An update to the 2007 review in Annals of Botany. *Ann. Bot.* **111**, 1021–1058 (2013).
4. S. Fonseca *et al.*, (+)-7-iso-jasmonoyl-L-isoleucine is the endogenous bioactive jasmonate. *Nat. Chem. Biol.* **5**, 344–350 (2009).
5. A. Chini *et al.*, The JAZ family of repressors is the missing link in jasmonate signalling. *Nature* **448**, 666–671 (2007).
6. L. B. Sheard *et al.*, Jasmonate perception by inositol-phosphate-potentiated COI1-JAZ co-receptor. *Nature* **468**, 400–405 (2010).
7. B. Thines *et al.*, JAZ repressor proteins are targets of the SCF(COI1) complex during jasmonate signalling. *Nature* **448**, 661–665 (2007).
8. L. Katsir, A. L. Schilmiller, P. E. Staswick, S. Y. He, G. A. Howe, COI1 is a critical component of a receptor for jasmonate and the bacterial virulence factor coronatine. *Proc. Natl. Acad. Sci. U.S.A.* **105**, 7100–7105 (2008).
9. O. Lorenzo, J. M. Chico, J. J. Sánchez-Serrano, R. Solano, JASMONATE-INSENSITIVE1 encodes a MYC transcription factor essential to discriminate between different jasmonate-regulated defense responses in Arabidopsis. *Plant Cell* **16**, 1938–1950 (2004).
10. I. Monte *et al.*, Ligand-receptor co-evolution shaped the jasmonate pathway in land plants. *Nat. Chem. Biol.* **14**, 480–488 (2018).
11. I. Monte *et al.*, A single JAZ repressor controls the jasmonate pathway in *Marchantia polymorpha*. *Mol. Plant* **12**, 185–198 (2019).
12. M. Peñuelas *et al.*, Jasmonate-related MYC transcription factors are functionally conserved in *Marchantia polymorpha*. *Plant Cell* **31**, 2491–2509 (2019).
13. E. E. Farmer, C. Davoine, Reactive electrophile species. *Curr. Opin. Plant Biol.* **10**, 380–386 (2007).
14. N. Taki *et al.*, 12-oxo-phytodienoic acid triggers expression of a distinct set of genes and plays a role in wound-induced gene expression in Arabidopsis. *Plant Physiol.* **139**, 1268–1283 (2005).
15. I. Monte *et al.*, An ancient COI1-independent function for reactive electrophilic oxylipins in thermotolerance. *Curr. Biol.* **30**, 962–971.e3 (2020).
16. H. Weber, B. A. Vick, E. E. Farmer, Dinor-oxo-phytodienoic acid: A new hexadecanoid signal in the jasmonate family. *Proc. Natl. Acad. Sci. U.S.A.* **94**, 10473–10478 (1997).
17. A. Schaller, A. Stintzi, Enzymes in jasmonate biosynthesis–structure, function, regulation. *Phytochemistry* **70**, 1532–1538 (2009).
18. F. Schaller, C. Biesgen, C. Müssig, T. Altmann, E. W. Weiler, 12-Oxophytodienoate reductase 3 (OPR3) is the isoenzyme involved in jasmonate biosynthesis. *Planta* **210**, 979–984 (2000).
19. A. Stintzi, J. Browse, The *Arabidopsis* male-sterile mutant, opr3, lacks the 12-oxophytodienoic acid reductase required for jasmonate synthesis. *Proc. Natl. Acad. Sci. U.S.A.* **97**, 10625–10630 (2000).
20. A. Chini *et al.*, An OPR3-independent pathway uses 4,5-didehydrojasmonate for jasmonate synthesis. *Nat. Chem. Biol.* **14**, 171–178 (2018).
21. P. E. Staswick, I. Tiryaki, The oxylipin signal jasmonic acid is activated by an enzyme that conjugates it to isoleucine in Arabidopsis. *Plant Cell* **16**, 2117–2127 (2004).
22. J. L. Bowman *et al.*, Insights into land plant evolution garnered from the *Marchantia polymorpha* genome. *Cell* **171**, 287–304.e15 (2017).
23. M. Stumpe *et al.*, The moss Physcomitrella patens contains cyclopentenones but no jasmonates: Mutations in allene oxide cyclase lead to reduced fertility and altered sporophyte morphology. *New Phytol.* **188**, 740–749 (2010).
24. G. Soriano *et al.*, An evolutionarily ancient fatty acid desaturase is required for the synthesis of hexadecatrienoic acid, which is the main source of the bioactive jasmonate in *Marchantia polymorpha*. *New Phytol.* **233**, 1401–1413 (2021).
25. M. Almeida-Trapp *et al.*, Development, validation, and application of an HPLC-MS/MS method for quantification of oxidized fatty acids in plants. *J. Chromatogr. B Analyt. Technol. Biomed. Life Sci.* **1186**, 123006 (2021).
26. J. L. Harwood, Recent advances in the biosynthesis of plant fatty acids. *Biochim. Biophys. Acta* **1301**, 7–56 (1996).
27. M. Kajikawa *et al.*, Production of arachidonic and eicosapentaenoic acids in plants using bryophyte fatty acid Delta6-desaturase, Delta6-elongase, and Delta5-desaturase genes. *Biosci. Biotechnol. Biochem.* **72**, 435–444 (2008).
28. I. Gill, R. Valivety, Polyunsaturated fatty acids. Part 1. Occurrence, biological activities and applications. *Trends Biotechnol.* **15**, 401–409 (1997).
29. Y. Lu, F. F. Eiriksson, M. Thorsteinsdóttir, H. T. Simonsen, Valuable fatty acids in bryophytes–production, biosynthesis, analysis and applications. *Plants* **8**, 1–18 (2019).
30. M. Cerone, T. K. Smith, A brief journey into the history of and future sources and uses of fatty acids. *Front. Nutr.* **8**, 570401 (2021).
31. I. A. Guschina, J. L. Harwood, Lipids and lipid metabolism in eukaryotic algae. *Prog. Lipid Res.* **45**, 160–186 (2006).
32. W. H. Gerwick, M. A. Roberts, A. Vulpanovici, D. L. Ballantine, Biogenesis and biological function of marine algal oxylipins. *Adv. Exp. Med. Biol.* **447**, 211–218 (1999).
33. K. Bouarab *et al.*, The innate immunity of a marine red alga involves oxylipins from both the eicosanoid and octadecanoid pathways. *Plant Physiol.* **135**, 1838–1848 (2004).
34. H. Kihara *et al.*, Arachidonic acid-dependent carbon-eight volatile synthesis from wounded liverwort (*Marchantia polymorpha*). *Phytochemistry* **107**, 42–49 (2014).
35. M. M. Tawfik, K. T. Yamato, T. Kohchi, T. Koeduka, K. Matsui, n-Hexanal and (Z)-3-hexenal are generated from arachidonic acid and linolenic acid by a lipoxygenase in *Marchantia polymorpha* L. *Biosci. Biotechnol. Biochem.* **81**, 1148–1155 (2017).
36. T. Albrecht *et al.*, Quantification of rapid, transient increases in jasmonic acid in wounded plants using a monoclonal antibody. *Planta* **191**, 86–94 (1993).
37. G. H. Jimenez-Aleman *et al.*, Omega hydroxylated JA-Ile is an endogenous bioactive jasmonate that signals through the canonical jasmonate signaling pathway. *Biochim. Biophys. Acta Mol. Cell Biol. Lipids* **1864**, 158520 (2019).
38. J. Ziegler, C. Wasternack, M. Hamberg, On the specificity of allene oxide cyclase. *Lipids* **34**, 1005–1015 (1999).
39. P. E. Staswick, W. Su, S. H. Howell, Methyl jasmonate inhibition of root growth and induction of a leaf protein are decreased in an *Arabidopsis thaliana* mutant. *Proc. Natl. Acad. Sci. U.S.A.* **89**, 6837–6840 (1992).
40. M. Takemura, T. Hamada, H. Kida, K. Ohyama, Cold-induced accumulation of ω-3 polyunsaturated fatty acid in a liverwort, *Marchantia polymorpha* L. *Biosci. Biotechnol. Biochem.* **76**, 785–790 (2012).
41. F. A. Ran *et al.*, Double nicking by RNA-guided CRISPR Cas9 for enhanced genome editing specificity. *Cell* **154**, 1380–1389 (2013).
42. S. S. Sugano *et al.*, CRISPR/Cas9-mediated targeted mutagenesis in the liverwort *Marchantia polymorpha* L. *Plant Cell Physiol.* **55**, 475–481 (2014).
43. A. V. Ogorodnikova *et al.*, Stereospecific biosynthesis of (9S,13S)-10-oxo-phytoenoic acid in young maize roots. *Biochim. Biophys. Acta* **1851**, 1262–1270 (2015).
44. S. A. Christensen *et al.*, Maize death acids, 9-lipoxygenase-derived cyclopente(a)nones, display activity as cytotoxic phytoalexins and transcriptional mediators. *Proc. Natl. Acad. Sci. U.S.A.* **112**, 11407–11412 (2015).
45. A. Redkar *et al.*, *Marchantia polymorpha* model reveals conserved infection mechanisms in the vascular wilt fungal pathogen *Fusarium oxysporum*. *New Phytol.* **234**, 227–241 (2021).
46. S. Gimenez-Ibanez, A. M. Zamarreño, J. M. García-Mina, R. Solano, An evolutionarily ancient immune system governs the interactions between *Pseudomonas syringae* and an early-diverging land plant lineage. *Curr. Biol.* **29**, 2270–2281.e4 (2019).
47. L. F. Thatcher, J. M. Manners, K. Kazan, *Fusarium oxysporum* hijacks COI1-mediated jasmonate signaling to promote disease development in *Arabidopsis*. *Plant J.* **58**, 927–939 (2009).
48. G.-Z. Han, Evolution of jasmonate biosynthesis and signaling mechanisms. *J. Exp. Bot.* **68**, 1323–1331 (2017).
49. M. He, C. X. Qin, X. Wang, N. Z. Ding, Plant unsaturated fatty acids: Biosynthesis and regulation. *Front Plant Sci* **11**, 390 (2020).
50. S. M. M. Shanab, R. M. Hafez, A. S. Fouad, A review on algae and plants as potential source of arachidonic acid. *J. Adv. Res.* **11**, 3–13 (2018).
51. N. Ruiz-Lopez, S. Usher, O. V. Sayanova, J. A. Napier, R. P. Haslam, Modifying the lipid content and composition of plant seeds: Engineering the production of LC-PUFA. *Appl. Microbiol. Biotechnol.* **99**, 143–154 (2015).
52. M. Schattat, K. Barton, B. Baudisch, R. B. Klösgen, J. Mathur, Plastid stromule branching coincides with contiguous endoplasmic reticulum dynamics. *Plant Physiol.* **155**, 1667–1677 (2011).
53. M. Morimoto, S. Kumeda, K. Komai, Insect antifeedant flavonoids from *Gnaphalium affine* D. Don. *J. Agric. Food Chem.* **48**, 1888–1891 (2000).
54. I. Heilmann, S. Mekhedov, B. King, J. Browse, J. Shanklin, Identification of the *Arabidopsis* palmitoyl-monogalactosyldiacylglycerol delta7-desaturase gene FAD5, and effects of plastidial retargeting of *Arabidopsis* desaturases on the fad5 mutant phenotype. *Plant Physiol.* **136**, 4237–4245 (2004).
55. A. J. K. Koo, X. Gao, A. D. Jones, G. A. Howe, A rapid wound signal activates the systemic synthesis of bioactive jasmonates in *Arabidopsis*. *Plant J.* **59**, 974–986 (2009).
56. G. Glauser *et al.*, Velocity estimates for signal propagation leading to systemic jasmonic acid accumulation in wounded Arabidopsis. *J. Biol. Chem.* **284**, 34506–34513 (2009).
57. A. Kimberlin, R. E. Holtsclaw, A. J. Koo, Differential regulation of the ribosomal association of mRNA transcripts in an *Arabidopsis* mutant defective in jasmonate-dependent wound response. *Front Plant Sci* **12**, 637959 (2021).
58. A. N. Poudel *et al.*, 12-hydroxy-jasmonoyl-l-isoleucine is an active jasmonate that signals through CORONATINE INSENSITIVE 1 and contributes to the wound response in *Arabidopsis*. *Plant Cell Physiol.* **60**, 2152–2166 (2019).
59. J. A. Napier, F. Beaudoin, L. V. Michaelson, O. Sayanova, The production of long chain polyunsaturated fatty acids in transgenic plants by reverse-engineering. *Biochimie* **86**, 785–792 (2004).
60. P. Da˛browska, D. Freitak, H. Vogel, D. G. Heckel, W. Boland, The phytohormone precursor OPDA is isomerized in the insect gut by a single, specific glutathione transferase. *Proc. Natl. Acad. Sci. U.S.A.* **106**, 16304–16309 (2009).
61. M. Shabab, S. A. Khan, H. Vogel, D. G. Heckel, W. Boland, OPDA isomerase GST16 is involved in phytohormone detoxification and insect development. *FEBS J.* **281**, 2769–2783 (2014).
62. R. Mittler, Oxidative stress, antioxidants and stress tolerance. *Trends Plant Sci.* **7**, 405–410 (2002).
63. C. H. Foyer, G. Noctor, Redox homeostasis and antioxidant signaling: A metabolic interface between stress perception and physiological responses. *Plant Cell* **17**, 1866–1875 (2005).
64. A. Delaunay-Moisan, C. Appenzeller-Herzog, The antioxidant machinery of the endoplasmic reticulum: Protection and signaling. *Free Radic. Biol. Med.* **83**, 341–351 (2015).
65. S. Kneeshaw *et al.*, Ligand diversity guarantees full activation of the jasmonate pathway in Marchantia polymorpha (RNA-Seq). NCBI GEO. https://www.ncbi.nlm.nih.gov/geo/query/acc.cgi?acc=GSE195837. Deposited 31 January 2022.
66. S. Kneeshaw *et al.*, Ligand diversity guarantees full activation of the jasmonate pathway in Marchantia polymorpha (array). NCBI GEO. https://www.ncbi.nlm.nih.gov/geo/query/acc.cgi?acc=GSE195838. Deposited 31 January 2022.
67. A. Kubota, K. Ishizaki, M. Hosaka, T. Kohchi, Efficient Agrobacterium-mediated transformation of the liverwort *Marchantia polymorpha* using regenerating thalli. *Biosci. Biotechnol. Biochem.* **77**, 167–172 (2013).
68. M. D. Robinson, D. J. McCarthy, G. K. Smyth, edgeR: A bioconductor package for differential expression analysis of digital gene expression data. *Bioinformatics* **26**, 139–140 (2010).